INTERNATIONAL JOURNAL FOR NUMERICAL METHODS IN ENGINEERING, VOL. 35, 521–539 (1992)

GRADIENT-DEPENDENT PLASTICITY: FORMULATION AND ALGORITHMIC ASPECTS

RENÉ DE BORST

Delft University of Technology, Department of Civil Engineering, TNO Building and Construction Research, P.O. Box 5048, 2600 GA Delft, The Netherlands

HANS-BERND MÜHLHAUS

CSIRO Division of Geomechanics, P.O. Box 54, Mt. Waverley, Vic. 3149, Australia

SUMMARY

A plasticity theory is proposed in which the yield strength not only depends on an equivalent plastic strain measure (hardening parameter), but also on the Laplacian thereof. The consistency condition now results in a differential equation instead of an algebraic equation as in conventional plasticity. To properly solve the set of non-linear differential equations the plastic multiplier is discretized in addition to the usual discretization of the displacements. For appropriate boundary conditions this formulation can also be derived from a variational principle. Accordingly, the theory is complete.

The addition of gradient terms becomes significant when modelling strain-softening solids. Classical models then result in loss of ellipticity of the governing set of partial differential equations. The addition of the gradient terms preserves ellipticity after the strain-softening regime has been entered. As a result, pathological mesh dependence as obtained in finite element computations with conventional continuum models is no longer encountered. This is demonstrated by some numerical simulations.

INTRODUCTION

Classical continuum models, i.e. continuum models that do not incorporate an internal length scale, suffer from pathological mesh dependence when strain-softening models are employed in numerical analyses. The underlying reason is that in this case the critical condition for localization coincides with the condition for loss of ellipticity of the governing differential equations. Consequently, the standard continuum theories commonly adopted to model localization leave the size of the localization zone unspecified.[1–6]

In contrast to conventional theories, higher-order continuum theories do not necessarily suffer from loss of ellipticity of the field equations when a strain-localization zone develops and are therefore able to provide meaningful numerical solutions of boundary-value problems involving strain softening and localization. In the past, various higher-order plasticity models have been suggested to model pattern formation and to regularize the governing field equations. Recent research suggests that especially the eighty-year-old Cosserat[7–10] theory and gradient plasticity theories[11–15] are well suited to achieve this objective.

While theoretically sound in the sense that these higher-order continuum theories result in a well-posed set of partial differential equations, the difficulties involved in producing solutions for these models seem almost insurmountable. This is true not only for analytical solutions, but also for numerical solutions, since established algorithms in computational plasticity cannot normally be transferred easily to higher-order plasticity models.

0029–5981/92/160521–19$14.50

Received 8 January 1991
Revised 29 October 1991

An exception is the Cosserat continuum. In this continuum model rotational degrees-of-freedom are added to the conventional translational degrees-of-freedom. Additional strain quantities (namely independent relative rotations and micro-curvatures) and additional stress quantities (couple-stresses) enter the continuum description as a result of this enhancement. It appears that the theory can be organized such that the classical format of computational plasticity can be recovered, enabling a straightforward use of the by now established concepts of return mapping and consistent tangent operators.[16-19] Use of this model yields efficient and fully mesh-independent solutions for static problems[5,6,10] as well as for dynamic problems.[20,21]

A problem with the Cosserat continuum, however, is that the rotational degrees-of-freedom are activated only under shear loadings. In pure (mode-I) tension rotational degrees-of-freedom do not become active, the micro-curvatures remain zero and accordingly also the couple-stresses. Although pure mode-I problems are of academic rather than of practical interest, and although all external actions on a structure generally result in a combination of mode-I (tension) and mode-II (shear) behaviour, numerical experiments suggest that, when decohesion is the predominant failure mode rather than frictional slip, the Cosserat effect is generally too weak to preserve ellipticity of the boundary-value problem. For this reason other possible enhancements of the conventional continuum should be investigated.

In the present contribution we shall utilize one such class of models, namely the gradient approach in which spatial derivatives of the inelastic state variables enter the constitutive description of the solid apart from the inelastic state variables themselves. Such models have been considered actively by others,[12-15] but a general methodology to incorporate such dependencies in a proper numerical strategy has not been presented hitherto. Previous numerical results were confined to one-dimensional applications[1,2,13,15] and the algorithms used to solve the boundary-value problems cannot readily be extended to more dimensions. In this article we shall propose and use such a general methodology in a finite element context. In this approach the notion is abandoned that, within the setting of a displacement-based finite element approach, the constitutive equations and the kinematic relations can be enforced in a strong sense, and that only equilibrium has to be satisfied in a weak sense. Instead, the key idea is introduced that the part of the constitutive equations that governs the evolution of the inelastic state variables is also satisfied only in a weak sense. For the case of a plasticity theory, as will be elaborated in this paper, this proposal implies that the yield condition is satisfied in a distributed sense, rather than pointwise. While in a conventional continuum little advantage seems to be gained, it seems a most natural approach when gradient or non-local continuum models are considered. In fact, the conclusion that in a non-local continuum the consistency condition can no longer be satisfied in a pointwise fashion was reached before, amongst others, by Simo.[22]

The paper is organized as follows. First the governing differential equations of an elasto-plastic continuum are derived in which the yield function not only depends on the stress tensor and a scalar-valued hardening parameter, but also on the Laplacian of the latter quantity. By resorting to the variational principle for gradient plasticity recently proposed by Mühlhaus and Aifantis,[11] it is shown that the theory is complete, including a proper formulation of the appropriate boundary conditions. It is also argued that, because of the dependence of the yield strength on the spatial gradients of the equivalent plastic strain measure, higher-order continuity requirements are imposed on the discretization of the plastic multiplier. Next a consistent treatment of the governing equations for finite increments of stress and strain is laid out. Finally the example of a bar loaded in uniaxial tension is considered. Analytical as well as numerical results are presented. The numerical results converge towards the analytical solution, both with respect to the load–displacement curve as well as with respect to the analytically predicted width of the localization zone.

FORMULATION OF A GRADIENT-DEPENDENT PLASTICITY MODEL

We consider the following set of equations:

$$\mathbf{L}^{\mathrm{T}}\dot{\boldsymbol{\sigma}} = \mathbf{0} \tag{1}$$

$$\dot{\boldsymbol{\sigma}} = \mathbf{D}[\dot{\boldsymbol{\varepsilon}} - \dot{\lambda}\mathbf{n}], \quad \dot{\lambda} \geqslant 0 \tag{2}$$

$$f(\boldsymbol{\sigma}, \kappa, \nabla^2\kappa) = 0 \tag{3}$$

$$\dot{\boldsymbol{\varepsilon}} = \mathbf{L}\dot{\mathbf{u}} \tag{4}$$

which define the elasto-plastic rate problem during continued yielding. In the equilibrium equation (1) $\boldsymbol{\sigma}$ is a vector that contains the stress components $(\sigma_{xx}, \sigma_{yy}, \sigma_{zz}, \sigma_{xy}, \sigma_{yz}, \sigma_{zx})$. The differential operator matrix $\mathbf{L}$ is then defined as

$$\mathbf{L} = \begin{bmatrix} \dfrac{\partial \cdot}{\partial x} & 0 & 0 \\ 0 & \dfrac{\partial \cdot}{\partial y} & 0 \\ 0 & 0 & \dfrac{\partial \cdot}{\partial z} \\ \dfrac{\partial \cdot}{\partial y} & \dfrac{\partial \cdot}{\partial x} & 0 \\ 0 & \dfrac{\partial \cdot}{\partial z} & \dfrac{\partial \cdot}{\partial y} \\ \dfrac{\partial \cdot}{\partial z} & 0 & \dfrac{\partial \cdot}{\partial x} \end{bmatrix} \tag{5}$$

and the superscript T is the transpose symbol. Under the assumption of small displacement gradients (which is made solely not to complicate the mathematical expressions unnecessarily) the operator matrix $\mathbf{L}$ can also be used to relate the strain components as assembled in the vector $\boldsymbol{\varepsilon} = (\varepsilon_{xx}, \varepsilon_{yy}, \varepsilon_{zz}, \gamma_{xy}, \gamma_{yz}, \gamma_{zx})$ to the displacement vector $\mathbf{u} = (u_x, u_y, u_z)$ in equation (4). As in classical plasticity, stress and the elastic strain $\dot{\boldsymbol{\varepsilon}}^{\mathrm{e}} = \dot{\boldsymbol{\varepsilon}} - \dot{\lambda}\mathbf{n}$ are related through the elastic rigidity matrix $\mathbf{D}$. The superimposed dots in equation (2) denote differentiation with respect to time. $\dot{\lambda}$ is a non-negative scalar-valued quantity which is a measure of the plastic flow intensity and $\mathbf{n}$ is the gradient to the yield surface as defined in (3):

$$\mathbf{n} = \frac{\partial f}{\partial \boldsymbol{\sigma}} \tag{6}$$

The salient feature of the plasticity theory which we shall consider in this article is the functional dependence of the yield function on the Laplacian of the hardening parameter κ in addition to the usual dependence of f on κ itself. The main departure from standard plasticity theory comes from the introduction of higher-order spatial gradients of the equivalent plastic strain in the yield criterion (3). Note that in the case of isotropy there must be even powers of the Laplacian. The only way to introduce the gradient of κ itself (in an isotropic medium) would be in a non-linear format, e.g. through $\sqrt{(\nabla\kappa)^{\mathrm{T}}\nabla\kappa}$. Formally the introduction of higher-order spatial gradients corresponds to a singular perturbation of the original yield criterion. The perturbation

terms are either thought to enrich the solution of the boundary-value problem by adding short-wavelength terms (if second- and fourth-order gradients are included), or are to stabilize the solution at a certain wavelength, set by the intrinsic length scale (second gradient only). The short-wavelength part may be periodic or of the boundary layer type, depending on the type of perturbation terms. Physically, the gradient terms imply or reflect the fact that below a certain size scale interaction between the microstructural carriers of the deformation is non-local. For a detailed discussion of non-local effects the reader is referred to the review paper by Kubin and Lépinoux.[23] A particularly convincing example of non-local hardening models, based on the interaction of a Frank–Read source with dipolar dislocation arrangements, can be found in the papers by Kratochvil,[24,25] whose work was again inspired by the reaction diffusion approach when modelling interactions between mobile and immobile dislocation species by Walgraef and Aifantis.[26] Furthermore, there is a non-local interaction between neighbouring slip planes by double cross-slip,[27,28] and in the context of granular materials the introduction of higher-order gradient terms has been motivated in Reference 10.

The dependence of the yield function on spatial gradients of an invariant measure of the plastic strain has a major impact when elaborating the condition that, during plastic flow, the stress point must remain on the yield surface:

$$\dot{f}(\boldsymbol{\sigma}, \kappa, \nabla^2\kappa) = 0 \tag{7}$$

which is commonly referred to as Prager's consistency condition. Taking into account the above dependencies equation (7) can be reworked to give

$$\mathbf{n}^{\mathrm{T}}\dot{\boldsymbol{\sigma}} + \frac{\partial f}{\partial \kappa}\dot{\kappa} + \frac{\partial f}{\partial \nabla^2 \kappa}\nabla^2\dot{\kappa} = 0 \tag{8}$$

Next the hardening modulus h is defined as in classical, gradient-independent plasticity:

$$h = -\frac{1}{\dot{\lambda}}\frac{\partial f}{\partial \kappa}\dot{\kappa} \tag{9}$$

so that the usual hardening diagram can be used. When the notation

$$\bar{c} = \frac{\partial f}{\partial \nabla^2 \kappa} \tag{10}$$

is adopted, equation (8) can be rewritten as

$$\mathbf{n}^{\mathrm{T}}\dot{\boldsymbol{\sigma}} - h\dot{\lambda} + \bar{c}\nabla^2\dot{\kappa} = 0 \tag{11}$$

In the following we assume $\bar{c}$ to be a constant for simplicity.

A further assumption that will be made at this point is that a relationship can be established between $\dot{\lambda}$ and $\dot{\kappa}$ of the form

$$\dot{\kappa} = \alpha\dot{\lambda} \tag{12}$$

with α a constant. This obviously limits the applicability of the theory somewhat. Nevertheless, large classes of hardening hypotheses and yield functions actually do result in a relationship as laid down in equation (12). For instance, for the von Mises yield function

$$f = \sqrt{3J_2} - \bar{\sigma}(\kappa, \nabla^2\kappa) \tag{13}$$

with J_2 the second invariant of the deviatoric stress tensor and $\bar{\sigma}$ the yield strength, and either the strain-hardening hypothesis

$$\dot{\kappa} = \sqrt{\tfrac{2}{3}(\dot{\boldsymbol{\varepsilon}}^{\mathrm{p}})^{\mathrm{T}}\dot{\boldsymbol{\varepsilon}}^{\mathrm{p}}} \tag{14}$$

or the work-hardening hypothesis

$$\dot{\kappa} = \boldsymbol{\sigma}^{\mathrm{T}}\dot{\boldsymbol{\varepsilon}}^{\mathrm{p}} \tag{15}$$

we obtain $\alpha = 1$. Similar results can be obtained for the Tresca yield function and the pressure-dependent Mohr–Coulomb and Drucker–Prager yield functions, provided that the softening mechanism is assumed to affect the cohesion and not the amount of friction that can be mobilized. It is thus believed that the above assumption does not significantly narrow the realm of application, while, if necessary, the theory can be extended to cases that α is not a constant. However, more complicated expressions than

$$\mathbf{n}^{\mathrm{T}}\dot{\boldsymbol{\sigma}} - h\dot{\lambda} + c\nabla^2\dot{\lambda} = 0 \tag{16}$$

which is obtained upon substitution of equation (12) in equation (11) and use of $c = \alpha\bar{c}$, then ensue.

We observe that, unlike conventional plasticity, the consistency condition results in a partial differential equation (16). This has the far-reaching consequence that an explicit expression for $\dot{\lambda}$ cannot be obtained at a local (integration point) level.

WEAK FORM OF THE FIELD EQUATIONS

While equations (1) and (16) describe incremental equilibrium and the evolution of the elasto-plastic process in a strong sense, a weak form of these rate equations is obtained by setting

$$\int_V \delta\dot{\mathbf{u}}^{\mathrm{T}}[\mathbf{L}^{\mathrm{T}}\dot{\boldsymbol{\sigma}}]\,\mathrm{d}V = 0 \tag{17}$$

and

$$\int_V \delta\dot{\lambda}[\mathbf{n}^{\mathrm{T}}\dot{\boldsymbol{\sigma}} - h\dot{\lambda} + c\nabla^2\dot{\lambda}]\,\mathrm{d}V = 0 \tag{18}$$

with the δ-symbol denoting the variation of a quantity. With aid of the divergence theorem equation (17) can be transformed as

$$\int_V \delta\dot{\boldsymbol{\varepsilon}}^{\mathrm{T}}\dot{\boldsymbol{\sigma}}\,\mathrm{d}V - \int_S \delta\dot{\mathbf{u}}^{\mathrm{T}}\dot{\mathbf{t}}\,\mathrm{d}S = 0 \tag{19}$$

with $\dot{\mathbf{t}}$ the rate of the tractions at the stress boundary. Substitution of the relationship between stress rate and the elastic part of the total strain rate, equation (2), in equations (18) and (19) subsequently leads to

$$\int_V \delta\dot{\boldsymbol{\varepsilon}}^{\mathrm{T}}\mathbf{D}(\dot{\boldsymbol{\varepsilon}} - \dot{\lambda}\mathbf{n})\,\mathrm{d}V - \int_S \delta\dot{\mathbf{u}}^{\mathrm{T}}\dot{\mathbf{t}}\,\mathrm{d}S = 0 \tag{20}$$

and

$$\int_V \delta\dot{\lambda}[\mathbf{n}^{\mathrm{T}}\mathbf{D}\dot{\boldsymbol{\varepsilon}} - (h + \mathbf{n}^{\mathrm{T}}\mathbf{D}\mathbf{n})\dot{\lambda} + c\nabla^2\dot{\lambda}]\,\mathrm{d}V = 0 \tag{21}$$

It is emphasized that, in contrast to the conventional approach in computational plasticity, the plastic multiplier $\dot{\lambda}$ is taken as an *independent* variable. While this approach is, in principle, also possible in gradient-independent plasticity it does not seem to entail major advantages when compared with the return-mapping algorithms.[16-18] For gradient plasticity, i.e. when $c \neq 0$ in equation (21), however, the discretization of λ seems natural and automatically gives satisfaction of the consistency condition in a distributed sense, cf. Simo.[22]

We now proceed in the usual manner, namely by discretizing the continuous displacement field $\mathbf{u}$ as

$$\mathbf{u} = \mathbf{H}\mathbf{a} \tag{22}$$

with $\mathbf{H}$ a matrix that contains the interpolation polynomials and $\mathbf{a}$ the nodal displacement vector. Combining equations (4) and (22) and introducing the matrix

$$\mathbf{B} = \mathbf{L}\mathbf{H} \tag{23}$$

the following relation between strain and nodal displacements is obtained:

$$\boldsymbol{\varepsilon} = \mathbf{B}\mathbf{a} \tag{24}$$

In a similar fashion the plastic multiplier $\dot{\lambda}$ can be discretized:

$$\dot{\lambda} = \mathbf{h}^{\mathrm{T}}\dot{\boldsymbol{\Lambda}} \tag{25}$$

and, since the Laplacian operator of $\dot{\lambda}$ must also be computed, the differential operator vector $\mathbf{p}$ is introduced:

$$\nabla^2\dot{\lambda} = \mathbf{p}^{\mathrm{T}}\dot{\boldsymbol{\Lambda}} \tag{26}$$

If $h_1, \ldots, h_n$ are the shape functions for the interpolation of the plastic multiplier, $\mathbf{p}$ is defined by

$$\mathbf{p} = [\nabla^2 h_1, \ldots, \nabla^2 h_n]^{\mathrm{T}} \tag{27}$$

Generally, the vector $\mathbf{h}$ will not contain the same interpolation polynomials as $\mathbf{H}$. While the interpolation of the displacement degrees-of-freedom requires only C^0-continuity, the fact that second derivatives of $\dot{\lambda}$ enter the weak form of the consistency condition makes it necessary to select C^1-continuous shape functions for the interpolation of $\dot{\lambda}$. For instance, for the one-dimensional examples that will be treated in a subsequent section, a Hermitian interpolation is employed for $\dot{\lambda}$ and linear interpolation is used for u_x, quite similar to beam-column elements where the interpolation of the transverse displacements is usually also achieved through Hermitian shape functions and the axial displacements are interpolated linearly.

Next we substitute equations (22), (24) and (25) in equation (20). The result is

$$\delta\dot{\mathbf{a}}^{\mathrm{T}} \int_V [\mathbf{B}^{\mathrm{T}}\mathbf{D}\mathbf{B}\dot{\mathbf{a}} - \mathbf{B}^{\mathrm{T}}\mathbf{D}\mathbf{n}\mathbf{h}^{\mathrm{T}}\dot{\boldsymbol{\Lambda}}]\,\mathrm{d}V - \delta\dot{\mathbf{a}}^{\mathrm{T}} \int_S \mathbf{H}^{\mathrm{T}}\dot{\mathbf{t}}\,\mathrm{d}S = 0 \tag{28}$$

Since this identity must hold for any admissible $\delta\dot{\mathbf{a}}$ the following set of algebraic equations ensues:

$$\int_V [\mathbf{B}^{\mathrm{T}}\mathbf{D}\mathbf{B}\dot{\mathbf{a}} - \mathbf{B}^{\mathrm{T}}\mathbf{D}\mathbf{n}\mathbf{h}^{\mathrm{T}}\dot{\boldsymbol{\Lambda}}]\,\mathrm{d}V = \int_S \mathbf{H}^{\mathrm{T}}\dot{\mathbf{t}}\,\mathrm{d}S \tag{29}$$

A similar operation on equation (21) results in

$$\delta\dot{\boldsymbol{\Lambda}}^{\mathrm{T}} \int_V [-\mathbf{h}\mathbf{n}^{\mathrm{T}}\mathbf{D}\mathbf{B}\dot{\mathbf{a}} + (h + \mathbf{n}^{\mathrm{T}}\mathbf{D}\mathbf{n})\mathbf{h}\mathbf{h}^{\mathrm{T}}\dot{\boldsymbol{\Lambda}} - c\mathbf{h}\mathbf{p}^{\mathrm{T}}\dot{\boldsymbol{\Lambda}}]\,\mathrm{d}V = 0 \tag{30}$$

and, by requiring that equation (30) must hold for all admissible $\delta\dot{\boldsymbol{\Lambda}}$, subsequently in

$$\int_V [-\mathbf{h}\mathbf{n}^T\mathbf{D}\mathbf{B}\dot{\mathbf{a}} + (h + \mathbf{n}^T\mathbf{D}\mathbf{n})\mathbf{h}\mathbf{h}^T\dot{\boldsymbol{\Lambda}} - c\mathbf{h}\mathbf{p}^T\dot{\boldsymbol{\Lambda}}]\,dV = \mathbf{0} \tag{31}$$

Equations (29) and (31) can be written in a compact fashion as

$$\begin{bmatrix} \mathbf{K}_{aa} & \mathbf{K}_{a\lambda} \\ \mathbf{K}_{a\lambda}^T & \mathbf{K}_{\lambda\lambda} \end{bmatrix} \begin{bmatrix} \dot{\mathbf{a}} \\ \dot{\boldsymbol{\Lambda}} \end{bmatrix} = \begin{bmatrix} \mathbf{f}_e \\ \mathbf{0} \end{bmatrix} \tag{32}$$

where

$$\mathbf{K}_{aa} = \int_V \mathbf{B}^T\mathbf{D}\mathbf{B}\,dV \tag{33}$$

$$\mathbf{K}_{a\lambda} = -\int_V \mathbf{B}^T\mathbf{D}\mathbf{n}\mathbf{h}^T dV \tag{34}$$

$$\mathbf{K}_{\lambda\lambda} = \int_V [(h + \mathbf{n}^T\mathbf{D}\mathbf{n})\mathbf{h}\mathbf{h}^T - c\mathbf{h}\mathbf{p}^T]\,dV \tag{35}$$

and the external force vector

$$\mathbf{f}_e = \int_S \mathbf{H}^T\mathbf{t}\,dS \tag{36}$$

Evidently the tangent stiffness matrix as defined in equations (32)–(35) is non-symmetric. This is solely due to the fact that gradient terms have entered the constitutive relationship. If $c = 0$ in equation (35) the non-symmetry disappears. We retrieve a symmetric operator as one would expect in classical plasticity with an associated flow rule (6).

For the pure rate problem as considered in this section the non-symmetric tangent operator defined in equations (32)–(35) can be symmetrized. However, when we consider finite loading steps, this is not possible and symmetrization of equation (35) therefore does not seem to offer much practical advantage. The main significance is that the present formulation, which sets out from a weak formulation of the evolution equation for the inelastic state variables, can be shown to be identical to the formulation that arises upon application of the variational principle for gradient plasticity, recently proposed by Mühlhaus and Aifantis[11] (for a brief summary the reader is referred to the Appendix). The other advantage is that the role of the additional boundary condition on $\dot{\lambda}$ is elucidated. For this discussion it is sufficient to consider only the last term of equation (35), or, more conveniently, equation (18). Application of Green's theorem to this term yields

$$\int_V c\delta\dot{\lambda}\nabla^2\dot{\lambda}\,dV = -\int_V c(\nabla\delta\dot{\lambda})^T(\nabla\dot{\lambda})\,dV + \int_{S_\lambda} c\delta\dot{\lambda}(\nabla\dot{\lambda})^T\mathbf{n}_\lambda\,dS_\lambda \tag{37}$$

with $\mathbf{n}_\lambda$ the outward normal at the elastic–plastic boundary S_λ. From equation (37) it follows that the condition on $\dot{\lambda}$ at the boundary of the plastically deforming part of the body must either be

$$\delta\dot{\lambda} = 0 \quad \text{or} \quad (\nabla\dot{\lambda})^T\mathbf{n}_\lambda = 0 \tag{38}$$

Equation (38.1) is automatically satisfied at each point of the (internal) elastic–plastic boundary in the interior of the body. When the spread of the plastic zone extends to an external boundary of the body either of conditions (38) may be imposed.

With equation (37) and assuming that the appropriate boundary conditions are satisfied $\mathbf{K}_{\lambda\lambda}$ can be written as

$$\mathbf{K}_{\lambda\lambda} = \int_V [(h + \mathbf{n}^T\mathbf{D}\mathbf{n})\mathbf{h}\mathbf{h}^T + c\mathbf{q}\mathbf{q}^T]\,dV \tag{39}$$

where

$$\mathbf{q} = [\nabla h_1, \ldots, \nabla h_n]^T \tag{40}$$

Comparing equation (32) containing $\mathbf{K}_{aa}$, $\mathbf{K}_{a\lambda}$ and $\mathbf{K}_{\lambda\lambda}$ as defined by equations (33), (34) and (39) with the tangent stiffness operator that follows from the variational principle of Mühlhaus and Aifantis,[11] shows that both formulations yield the same result for infinitesimally small load increments. When finitely sized loading steps are used this is no longer the case and the non-symmetric definition of equation (35) must be utilized to obtain proper convergence characteristics in an incremental-iterative procedure.

ALGORITHMIC ASPECTS

In order to devise a proper algorithm that enforces equilibrium and satisfaction of the yield function, albeit both in a distributed sense, at the end of every loading step, we set out to achieve that, at iteration $j + 1$ of the current loading step, we have

$$\mathbf{L}^T\boldsymbol{\sigma}_{j+1} = \mathbf{0} \tag{41}$$

and

$$f(\boldsymbol{\sigma}_{j+1}, \kappa_{j+1}, \nabla^2\kappa_{j+1}) = 0 \tag{42}$$

In the same way as in the preceding section we shall formulate the weak form of equations (41) and (42) as follows:

$$\int_V \delta\dot{\mathbf{u}}^T[\mathbf{L}^T\boldsymbol{\sigma}_{j+1}]\,dV = 0 \tag{43}$$

or, invoking the divergence theorem,

$$\int_V \delta\dot{\boldsymbol{\varepsilon}}^T\boldsymbol{\sigma}_{j+1}\,dV - \int_S \delta\dot{\mathbf{u}}^T\mathbf{t}_{j+1}\,dS = 0 \tag{44}$$

and

$$\int_V \delta\dot{\lambda} f(\boldsymbol{\sigma}_{j+1}, \kappa_{j+1}, \nabla^2\kappa_{j+1})\,dV = 0 \tag{45}$$

To arrive at a proper incremental-iterative procedure the stress at iteration $j + 1$ is decomposed into the stress at iteration j and the stress increment

$$d\boldsymbol{\sigma} = \boldsymbol{\sigma}_{j+1} - \boldsymbol{\sigma}_j \tag{46}$$

so that equation (44) changes into

$$\int_V \delta\dot{\boldsymbol{\varepsilon}}^T\mathbf{D}\,d\boldsymbol{\sigma}\,dV = \int_S \delta\dot{\mathbf{u}}^T\mathbf{t}_{j+1}\,dS - \int_V \delta\dot{\boldsymbol{\varepsilon}}^T\boldsymbol{\sigma}_j\,dV \tag{47}$$

Next, the yield function f is developed in a Taylor series that is truncated after the linear terms:

$$f(\boldsymbol{\sigma}_j, \kappa_j, \nabla^2\kappa_j) + \mathbf{n}_j^T\,d\boldsymbol{\sigma} - h\,d\lambda + c\nabla^2(d\lambda) = 0 \tag{48}$$

where $\mathbf{n}_j = \mathbf{n}(\boldsymbol{\sigma}_j)$ and

$$\mathrm{d}\lambda = \lambda_{j+1} - \lambda_j \tag{49}$$

and where it has been assumed that, in a spirit similar to that of the preceding section, $\mathrm{d}\kappa = \alpha \mathrm{d}\lambda$. With equation (48), equation (45) is modified to

$$\int_V \delta\dot{\lambda}[\mathbf{n}_j^{\mathrm{T}} \mathrm{d}\boldsymbol{\sigma} - h\mathrm{d}\lambda + c\nabla^2(\mathrm{d}\lambda)]\,\mathrm{d}V = -\int_V \delta\dot{\lambda} f(\boldsymbol{\sigma}_j, \kappa_j, \nabla^2\kappa_j)\,\mathrm{d}V \tag{50}$$

Substitution of the relationship between the stress increment and the elastic part of the strain increment,

$$\mathrm{d}\boldsymbol{\sigma} = \mathbf{D}(\mathrm{d}\boldsymbol{\varepsilon} - \mathrm{d}\lambda \mathbf{n}_j) \tag{51}$$

in equations (47) and (50), then leads to

$$\int_V \delta\dot{\boldsymbol{\varepsilon}}^{\mathrm{T}}(\mathbf{D}\mathrm{d}\boldsymbol{\varepsilon} - \mathrm{d}\lambda \mathbf{D}\mathbf{n}_j)\,\mathrm{d}V = \int_S \delta\dot{\mathbf{u}}^{\mathrm{T}}\mathbf{t}_{j+1}\,\mathrm{d}S - \int_V \delta\dot{\boldsymbol{\varepsilon}}^{\mathrm{T}}\boldsymbol{\sigma}_j\,\mathrm{d}V \tag{52}$$

and

$$\int_V \delta\dot{\lambda}[\mathbf{n}^{\mathrm{T}}\mathbf{D}\mathrm{d}\boldsymbol{\varepsilon} - (h + \mathbf{n}^{\mathrm{T}}\mathbf{D}\mathbf{n})\mathrm{d}\lambda + c\nabla^2(\mathrm{d}\lambda)]\,\mathrm{d}V = -\int_V \delta\dot{\lambda} f(\boldsymbol{\sigma}_j, \kappa_j, \nabla^2\kappa_j)\,\mathrm{d}V \tag{53}$$

Upon substitution of the analogue of equations (24) and (25) for finite increments in equations (52) and (53) we obtain

$$\delta\dot{\mathbf{a}}^{\mathrm{T}}\int_V [\mathbf{B}^{\mathrm{T}}\mathbf{D}\mathbf{B}\mathrm{d}\mathbf{a} - \mathbf{B}^{\mathrm{T}}\mathbf{D}\mathbf{n}\mathbf{h}^{\mathrm{T}}\mathrm{d}\Lambda]\,\mathrm{d}V = \delta\dot{\mathbf{a}}^{\mathrm{T}}\int_S \mathbf{H}^{\mathrm{T}}\mathbf{t}_{j+1}\,\mathrm{d}S - \delta\dot{\mathbf{a}}^{\mathrm{T}}\int_V \mathbf{B}^{\mathrm{T}}\boldsymbol{\sigma}_j\mathrm{d}V \tag{54}$$

and

$$\delta\dot{\boldsymbol{\Lambda}}^{\mathrm{T}}\int_V [-\mathbf{h}\mathbf{n}^{\mathrm{T}}\mathbf{D}\mathbf{B}\mathrm{d}\mathbf{a} + (h + \mathbf{n}^{\mathrm{T}}\mathbf{D}\mathbf{n})\mathbf{h}\mathbf{h}^{\mathrm{T}}\mathrm{d}\Lambda - c\mathbf{h}\mathbf{p}^{\mathrm{T}}\mathrm{d}\Lambda]\,\mathrm{d}V = \delta\dot{\boldsymbol{\Lambda}}^{\mathrm{T}}\int_V f(\boldsymbol{\sigma}_j, \kappa_j, \nabla^2\kappa_j)\mathbf{h}\,\mathrm{d}V \tag{55}$$

Since these identities must hold for any admissible $\delta\dot{\mathbf{a}}$ and $\delta\dot{\boldsymbol{\Lambda}}$ the following sets of algebraic equations ensue:

$$\int_V [\mathbf{B}^{\mathrm{T}}\mathbf{D}\mathbf{B}\mathrm{d}\mathbf{a} - \mathbf{B}^{\mathrm{T}}\mathbf{D}\mathbf{n}\mathbf{h}^{\mathrm{T}}\mathrm{d}\Lambda]\,\mathrm{d}V = \int_S \mathbf{H}^{\mathrm{T}}\mathbf{t}_{j+1}\,\mathrm{d}S - \int_V \mathbf{B}^{\mathrm{T}}\boldsymbol{\sigma}_j\mathrm{d}V \tag{56}$$

and

$$\int_V [-\mathbf{h}\mathbf{n}^{\mathrm{T}}\mathbf{D}\mathbf{B}\mathrm{d}\mathbf{a} + (h + \mathbf{n}^{\mathrm{T}}\mathbf{D}\mathbf{n})\mathbf{h}\mathbf{h}^{\mathrm{T}}\mathrm{d}\Lambda - c\mathbf{h}\mathbf{p}^{\mathrm{T}}\mathrm{d}\Lambda]\,\mathrm{d}V = \int_V f(\boldsymbol{\sigma}_j, \kappa_j, \nabla^2\kappa_j)\mathbf{h}\,\mathrm{d}V \tag{57}$$

Equations (56) and (57) can be written in a compact fashion as

$$\begin{bmatrix} \mathbf{K}_{aa} & \mathbf{K}_{a\lambda} \\ \mathbf{K}_{a\lambda}^{\mathrm{T}} & \mathbf{K}_{\lambda\lambda} \end{bmatrix}\begin{bmatrix} \mathrm{d}\mathbf{a} \\ \mathrm{d}\Lambda \end{bmatrix} = \begin{bmatrix} \mathbf{f}_c + \mathbf{f}_a \\ \mathbf{f}_\lambda \end{bmatrix} \tag{58}$$

where $\mathbf{K}_{aa}$, $\mathbf{K}_{a\lambda}$ and $\mathbf{K}_{\lambda\lambda}$ are defined in (33)–(35). $\mathbf{f}_a$ and $\mathbf{f}_\lambda$ are defined by

$$\mathbf{f}_a = -\int_V \mathbf{B}^{\mathrm{T}}\boldsymbol{\sigma}_j\mathrm{d}V \tag{59}$$

and

$$\mathbf{f}_\lambda = \int_V f(\boldsymbol{\sigma}_j, \kappa_j, \nabla^2 \kappa_j)\mathbf{h}\, \mathrm{d}V \tag{60}$$

The algorithm as described in the preceding equations is summarized in Box 1. Noteworthy is that the condition $f(\boldsymbol{\sigma}_j + \mathbf{D}\mathrm{d}\boldsymbol{\varepsilon}) \geqslant -\varepsilon$ is used to determine whether a point is in a plastic state. If this condition is not fulfilled elastic behaviour is assumed and an artificial hardening modulus $h = E^4$ is substituted in the next iteration to form the tangent operator in that particular integration point.

Instead of penalizing the hardening modulus by assigning it an artificially high value, degrees-of-freedom that correspond to the interpolation of $\dot{\lambda}$ can be omitted from the set of equations. This has two important drawbacks. Firstly, there is the issue of a constantly changing number of degrees-of-freedom, as even between two consecutive iterations points may change from an elastic state to a plastic state and vice versa. This is usually highly inconvenient when adapting existing

Box 1. Summary of algorithm for gradient von Mises plasticity

1. Compute $\mathbf{K}_{aa}$, $\mathbf{K}_{a\lambda}$, $\mathbf{K}_{\lambda\lambda}$, $\mathbf{f}_a$ and $\mathbf{f}_\lambda$ according to equations (33)–(36), (59) and (60)
2. Solve for $\mathrm{d}\mathbf{a}$ and $\mathrm{d}\boldsymbol{\Lambda}$ according to equation (58)

For each integration point:

3. Compute:
$$\mathrm{d}\boldsymbol{\varepsilon} = \mathbf{B}\mathrm{d}\mathbf{a}$$
$$\mathrm{d}\lambda = \mathbf{h}^{\mathrm{T}}\mathrm{d}\boldsymbol{\Lambda}$$
$$\nabla^2(\mathrm{d}\lambda) = \mathbf{p}^{\mathrm{T}}\mathrm{d}\boldsymbol{\Lambda}$$
4. Update:
$$\lambda_{j+1} = \lambda_j + \mathrm{d}\lambda$$
$$\nabla^2\lambda_{j+1} = \nabla^2\lambda_j + \nabla^2(\mathrm{d}\lambda)$$
5. Compute trial stress:
$$\boldsymbol{\sigma}_{\mathrm{trial}} = \boldsymbol{\sigma}_j + \mathbf{D}\mathrm{d}\boldsymbol{\varepsilon}$$
6. If $f(\boldsymbol{\sigma}_{\mathrm{trial}}, \lambda_{j+1}, \nabla^2\lambda_{j+1}) \geqslant -\varepsilon$

   then: $\boldsymbol{\sigma}_{j+1} = \boldsymbol{\sigma}_{\mathrm{trial}} - \mathrm{d}\lambda\mathbf{D}\mathbf{n}_j$

   compute h for next iteration

   else: $\boldsymbol{\sigma}_{j+1} = \boldsymbol{\sigma}_{\mathrm{trial}}$

   set $h = E^4$ for next iteration
7. Check $f(\boldsymbol{\sigma}_{j+1}, \lambda_{j+1}, \nabla^2\lambda_{j+1}) \geqslant -\varepsilon$

   If this condition is violated, compute R such that
$$f(\boldsymbol{\sigma}_{\mathrm{trial}} - R\mathrm{d}\lambda\mathbf{D}\mathbf{n}_j, \lambda_{j+1}, \nabla^2\lambda_{j+1}) \geqslant -\varepsilon$$
$$\lambda_{j+1} = \lambda_j + R\mathrm{d}\lambda$$
$$\nabla^2\lambda_{j+1} = \nabla^2\lambda_j + R\nabla^2(\mathrm{d}\lambda)$$
8. Check global convergence criterion. If not converged, go to 1

finite element codes. Secondly, the extent of the plastic region is monitored at the Gauss points, which do not coincide with the nodes. It is not straightforward to determine which nodal degrees-of-freedom for the interpolation of $\dot{\lambda}$ must be made active and inactive, respectively, when the plasticity status in one or more integration points of an element changes.

Finally, it is emphasized again that the current formulation does not satisfy the yield condition $f = 0$ in a pointwise fashion, but merely in a distributed sense. Moreover, the latter condition, namely $\int \delta\dot{\lambda} f(\boldsymbol{\sigma}, \kappa, \nabla^2\kappa) \mathrm{d}V = 0$, is not satisfied at each iteration, but only at the end of a loading step. This is because $\dot{\lambda}$ is taken as an independent variable and is included in the solution process at global, structural level. For gradient plasticity this is inevitable. For local plasticity formulations the by now established return-mapping algorithms are probably as good as the current formulation, while being simpler in the sense that they do not carry the overhead of including $\dot{\lambda}$ as an independent variable at global level. Nevertheless, for gradient-independent plasticity the proposed procedure can be related to return-mapping approaches in the sense that for homogeneous stress states the algorithm reduces to the Tangent Cutting Plane algorithm proposed by Ortiz and Simo.[17]

EXAMPLE

Problem statement

The model problem that we shall consider to test our solution strategy for gradient plasticity is depicted in Figure 1. It is a one-dimensional bar of length L that is loaded in pure tension. In the elastic regime Young's modulus E governs the relation between stress and strain: $\sigma = E\varepsilon$. When the maximum tensile strength σ_t is attained softening occurs according to the linear diagram of Figure 2. For this situation a second-order gradient plasticity theory can be summarized by the set of equations

$$f = \sigma - \bar{\sigma}\left(\varepsilon^p, \frac{\mathrm{d}^2\varepsilon^p}{\mathrm{d}x^2}\right) \tag{61}$$

and

$$\bar{\sigma} = \sigma_t + h\varepsilon^p - c\frac{\mathrm{d}^2\varepsilon^p}{\mathrm{d}x^2} \tag{62}$$

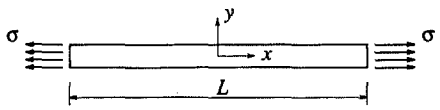

Figure 1. Bar with length L subjected to an axial stress σ

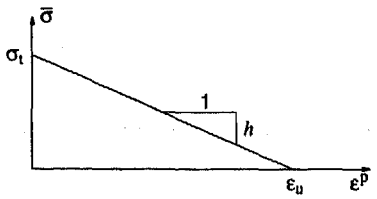

Figure 2. Linear softening diagram for local action in gradient plasticity

with ε^p the plastic strain. For the linear softening diagram h will have a negative, constant value. Note that the restriction that h is a constant implies that the solution that will be derived below ceases to be valid if ε^p exceeds the strain $\varepsilon_u = -h^{-1}\sigma_t$ at which the stress due to the local effect has come down to zero (Figure 2). Also c is assumed to have a constant value, although the numerical simulations to be presented in the following suggest that this is probably not a very appropriate choice. Finally, the boundary condition

$$\dot{\varepsilon}^p = 0 \tag{63}$$

is imposed at the elastic–plastic boundary.

Analytical solution

From equation (62) we can derive that the solution for ε^p has the form

$$\varepsilon^p = A\cos(x/l) + h^{-1}(\bar{\sigma} - \sigma_t) \tag{64}$$

with A an integration constant, and

$$l = \sqrt{-\frac{c}{h}} \tag{65}$$

For softening $h < 0$, so that c must be positive in order that equations (64) and (65) make sense. For the general case of a three-dimensional continuum this observation was also made by Mühlhaus and Aifantis.[11] Furthermore, l has the dimension of length. Accordingly, an internal length scale is present in our continuum model.

Differentiation of equation (64) with respect to the time gives for the plastic strain rate

$$\dot{\varepsilon}^p = \dot{A}\cos(x/l) + h^{-1}\dot{\sigma} \tag{66}$$

where equation (61) and the fact that $\dot{f} = 0$ during continued plastic flow have been utilized. Suppose that the plastic zone has a width w. Application of the boundary condition (63) at $x = w/2$ (elastic–plastic boundary) then results in

$$\dot{\varepsilon}^p = \frac{\dot{\sigma}}{h}\left[1 - \frac{\cos(x/l)}{\cos(w/(2l))}\right] \tag{67}$$

Addition of the elastic strain rate $\dot{\varepsilon}^e = \dot{\sigma}/E$ results in

$$\dot{\varepsilon} = \frac{\dot{\sigma}}{E} + \frac{\dot{\sigma}}{h}\left[1 - \frac{\cos(x/l)}{\cos(w/(2l))}\right] \tag{68}$$

so that the velocity at the elastic–plastic boundary ($x = w/2$) is given by

$$\dot{u}(w/2) = \frac{\dot{\sigma}w}{2E} + \frac{\dot{\sigma}}{h}\int_0^{w/2}\left[1 - \frac{\cos(x/l)}{\cos(w/(2l))}\right]\mathrm{d}x \tag{69}$$

Integration of equation (69) and addition of the velocity in the elastic part of the bar (from $x = w/2$ to $x = L/2$) results in the following expression for the velocity at the right end of the bar:

$$\frac{\dot{u}(L/2)}{\dot{\sigma}} = \frac{L}{2E} + \frac{1}{h}[w/2 - l\tan(w/(2l))] \tag{70}$$

We are now interested in the aperiodic solution that results in the steepest descending branch, i.e. the most critical equilibrium path. This solution is obtained by requiring that

$$\frac{\mathrm{d}(\dot{u}(L/2)/\dot{\sigma})}{\mathrm{d}(w/2)} = 0 \tag{71}$$

Imposing this requirement results in

$$\cos^2(w/(2l)) = 1 \tag{72}$$

The smallest non-trivial argument that satisfies equation (72) is π, so that

$$w = 2\pi\sqrt{-\frac{c}{h}} \tag{73}$$

which, for a steady-state solution, establishes a relation between the width of the localization zone w and the model parameters h and c.

Substitution of equation (73) in equation (70) now results in the following expression for the relation between the velocity of the right end of the bar and the stress rate:

$$\frac{\dot{u}(L/2)}{\dot{\sigma}} = \frac{L}{2E} + \frac{w}{2h} \tag{74}$$

The relation between the difference in velocities of both ends of the bar, $\Delta\dot{u} = \dot{u}(L/2) - \dot{u}(-L/2)$, and the stress rate then becomes

$$\frac{\Delta\dot{u}}{\dot{\sigma}} = \frac{L}{E} + \frac{w}{h} \tag{75}$$

The above analytical solution shows, firstly, that the width of the localization zone is fully determined by the model parameters h and c, and secondly, that the length of the bar, L, enters the expression for the slope of the stress–displacement curve. The latter property implies that a size effect is incorporated in the model. Indeed, if L is made larger the ratio $\Delta\dot{u}/\dot{\sigma}$ becomes smaller, so that a more brittle post-peak behaviour is predicted. For $L > -wE/h$ we even obtain snap-back behaviour.

Numerical results

As an example a bar with a length $L = 100$ mm is taken. A Young's modulus $E = 20\,000$ N/mm^2 is used for the entire bar. The initial tensile strength is $\sigma_t = 2$ N/mm^2 except for the elements which are between $x = 45$ and $x = 55$ mm. For these elements the initial tensile strength has been reduced by 10 per cent. After reaching the peak strength a softening modulus $h = -0{\cdot}1E$ is used for all elements, including the weakened elements. When the ultimate tensile strain $\varepsilon_u = 10^{-3}$ (Figure 2) has been reached at which the residual load-carrying capacity has been reduced to zero the stress due to local softening is kept at that value, so that the softening modulus also becomes zero.

The reference solution has been carried out for a value of the internal length parameter of $l = 5$ mm. The numerical solutions show that upon mesh refinement the width of the localization zone and the strain profile over this zone rapidly converge towards a unique value. This is shown in Figures 3 and 4, in which the plastic and the total strain distributions along the axis of the bar have been plotted for $\Delta u = 0{\cdot}02$ mm. While the strain profiles of the solution for 20 elements still deviate somewhat, the solutions for 40, 80 and 160 elements are very similar. For these

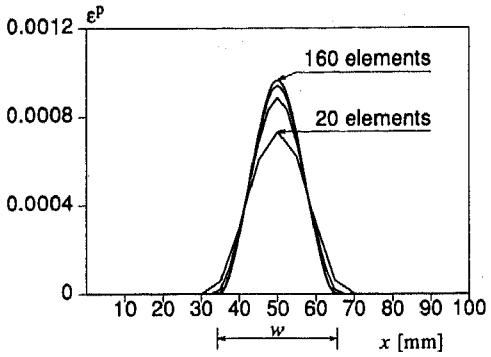

Figure 3. Plastic strain distribution along the axis of a tension bar with an imperfection at the centre for different discretizations ($l/L = 0{\cdot}05$ and $\Delta u = 0{\cdot}02$)

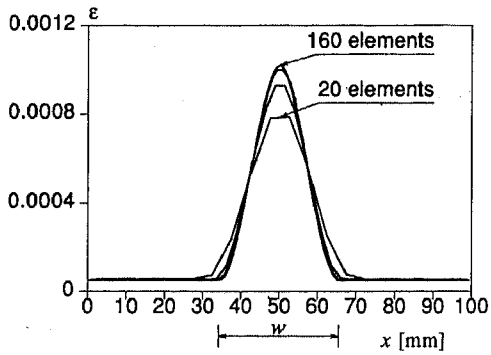

Figure 4. Total strain distribution along the axis of a tension bar with an imperfection at the centre for different discretizations ($l/L = 0{\cdot}05$ and $\Delta u = 0{\cdot}02$)

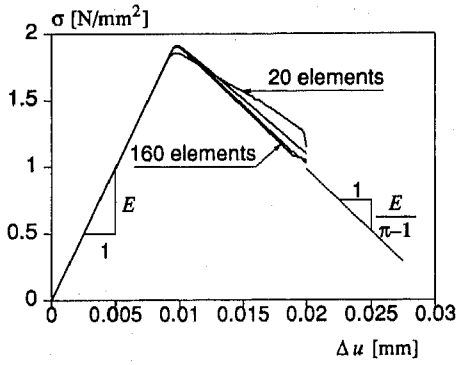

Figure 5. Axial stress vs difference in axial displacements of both ends of a tension bar with an imperfection at the centre ($l/L = 0{\cdot}05$)

discretizations the cosine distribution for the plastic strains that is predicted by the analytical solution also comes out nicely.

Figure 5 shows the convergence of the load–displacement curves. Again the solution for 20 elements is still slightly stiff, but the solutions for the discretizations with 40, 80 and 160 elements agree well, not only mutually, but also with the analytical solution. For the present geometry and set of material parameters ($l = 5$ mm) equation (75) gives

$$\frac{\Delta \dot{u}/L}{\dot{\sigma}} = \frac{1}{E}(1 - \pi) \tag{76}$$

Especially the results for the meshes with 80 and 160 elements match the analytical solution perfectly.

All numerical solutions correspond to perfectly converged equilibrium states (force norm 10^{-6}). When the steady-state solution has developed the problem is linear until the strain ε_u is reached in the centre of the bar. Indeed, in this part of the localization process only one iteration with a tangent operator is needed to achieve equilibrium.

For the mesh with 160 elements the problem has also been analysed for $l = 2{\cdot}5$ and $l = 10$ mm. The load–displacement curves are given in Figure 6. It is interesting to observe that for a residual stress level $\sigma \approx 1\text{N/mm}^2$ the load–displacement curves for $l = 2{\cdot}5$ and $l = 5$ mm show a rather sharp cusp. At this point the centre two integration points exit from the softening part of the local stress–strain diagram. All residual load-carrying capacity in these integration points is then due to the gradient effect. The zone in which all load-carrying capacity is due to the gradient effect gradually grows from this point onwards until a new steady-state situation is attained where the residual stress level becomes constant. Indeed, when c is rigorously assigned a constant value and if h is set equal to zero, equation (75) predicts that $\dot{\sigma} \to 0$ and the stress–displacement curve converges towards a horizontal asymptote. To avoid that even in pure tension a steady-state solution is reached at a non-zero residual stress level, c would have to be made a function of κ: $c = c(\kappa)$.

Figures 7 illustrate the gradual growth of the localization zone for a division of the bar into 160 elements. For $l = 2{\cdot}5$, $l = 5$ and $l = 10$ mm the plastic strain distribution has been plotted for $\Delta u = 0{\cdot}01$, $0{\cdot}0125$, $0{\cdot}015$ and $0{\cdot}02$ mm respectively. In Figure 7(c) the plastic strain distribution is also shown for $\Delta u = 0{\cdot}03$ mm ($l/L = 0{\cdot}1$). The numerical solutions show that, starting from the initial imperfect elements, a localization zone grows gradually until the analytically predicted widths are reached.

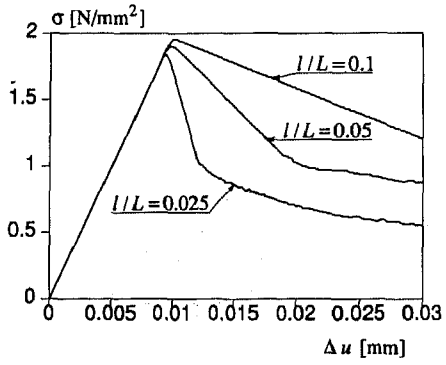

Figure 6. Axial stress vs difference in axial displacements of both ends of a tension bar with an imperfection at the centre for different ratios of l/L (all results are for 160 elements)

CONCLUDING REMARKS

A plasticity theory has been proposed that includes a dependence upon the second gradient of an invariant measure of the inelastic strain. The model thus obtained has the favourable property that the governing set of partial differential equations remains elliptic after the onset of localization. This ensures that meaningful solutions are obtained both analytically and numerically. For the simple boundary value of a bar loaded in uniaxial tension this has been demonstrated rigorously.

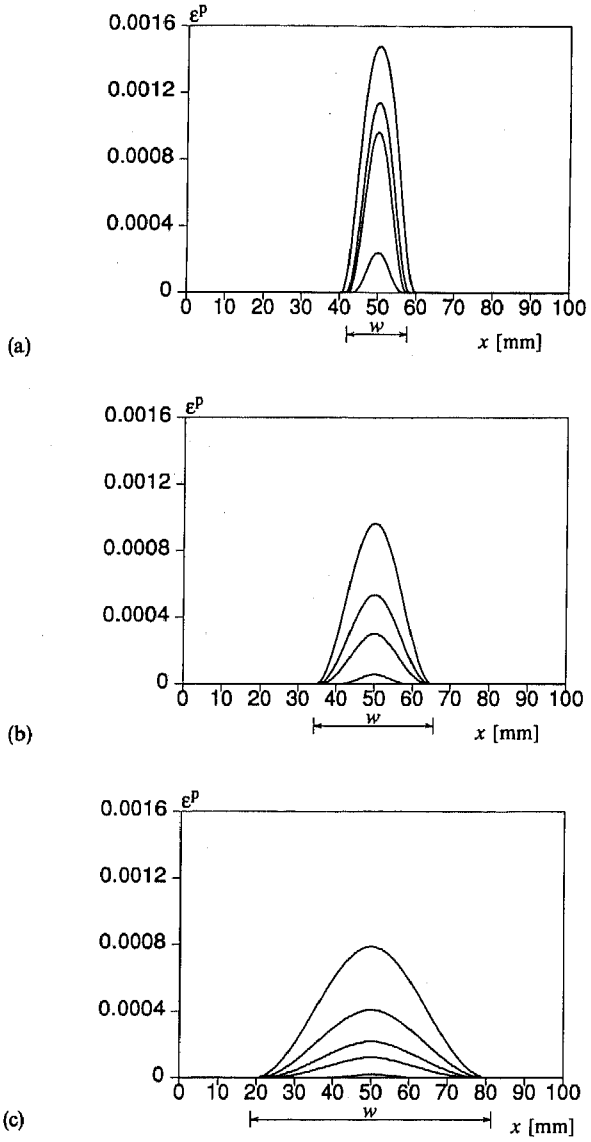

Figure 7. Evolution of the plastic strain distribution along the axis of a tension bar with an imperfection at the centre: (a) $l/L = 0{\cdot}025$; (b) $l/L = 0{\cdot}05$; (c) $l/L = 0{\cdot}1$

The major novel aspect of the present study is that the inelastic variables (in the present case: the plastic multiplier) are considered as independent variables. Hence, these variables are interpolated separately from the displacements. While not much seems to be gained in conventional plasticity it is a very natural approach for gradient or non-local plasticity and ensures satisfaction of the consistency and yield conditions in a distributed sense.[22]

For appropriate boundary conditions the pure rate problem can also be derived from a variational principle.[11] This explicit consideration of the boundary conditions ensures that the theory is complete.

The present gradient plasticity theory can be used for degrading materials in which the prevailing failure mechanism is frictional slip and for materials in which decohesion plays a predominant role. For the latter category of materials the present approach seems better suited than the Cosserat continuum model, which has proved very appropriate to analyse materials in which frictional slip plays an important role, e.g. sand.[8-10]

A disadvantage of the gradient model is the smoothness requirement on the interpolation of the inelastic state variable. For instance, the second-order gradient plasticity theory as used here necessitates C^1-continuity of the interpolation functions for the plastic multiplier $\dot{\lambda}$.

ACKNOWLEDGEMENTS

Financial support by CUR-committee A30 'Concrete Mechanics' and by the Commission of the European Communities through the Brite-Euram Programme (Project BE–89-3275) to the first author is gratefully acknowledged.

APPENDIX

We consider the following functional:[11]

$$F(\dot{\mathbf{u}}, \dot{\lambda}) = \frac{1}{2}\int_V [(\dot{\boldsymbol{\varepsilon}} - \dot{\lambda}\mathbf{n})^T\mathbf{D}(\dot{\boldsymbol{\varepsilon}} - \dot{\lambda}\mathbf{n}) + h\dot{\lambda}^2 + c(\nabla\dot{\lambda})^T(\nabla\dot{\lambda})]\,dV - \int_S \dot{\mathbf{u}}^T\dot{\mathbf{t}}\,dS \tag{77}$$

subject to the constraint $\dot{\lambda} \geqslant 0$. In equation (77) all symbols have the same meaning as in the body of the paper. Substitution of the strain–nodal displacement relation (24), the interpolations (22) and (25), and equation (40) results in

$$F(\dot{\mathbf{a}}, \dot{\mathbf{A}}) = \frac{1}{2}\int_V [(\mathbf{B}\dot{\mathbf{a}} - \mathbf{n}\mathbf{h}^T\dot{\mathbf{A}})^T\mathbf{D}(\mathbf{B}\dot{\mathbf{a}} - \mathbf{n}\mathbf{h}^T\dot{\mathbf{A}}) + h(\mathbf{h}^T\dot{\mathbf{A}})^2 + c(\mathbf{q}^T\dot{\mathbf{A}})^2]\,dV - \int_S \dot{\mathbf{a}}^T\mathbf{H}^T\mathbf{t}\,dS \tag{78}$$

Differentiation with respect to $\dot{\mathbf{a}}$ and $\dot{\mathbf{A}}$ respectively yields

$$\frac{\partial F}{\partial \dot{\mathbf{a}}} = \int_V [\mathbf{B}^T\mathbf{D}\mathbf{B}\dot{\mathbf{a}} - \mathbf{B}^T\mathbf{D}\mathbf{n}\mathbf{h}^T\dot{\mathbf{A}}]\,dV - \int_S \mathbf{H}^T\dot{\mathbf{t}}\,dS \tag{79}$$

$$\frac{\partial F}{\partial \dot{\mathbf{A}}} = \int_V [-\mathbf{h}\mathbf{n}^T\mathbf{D}\mathbf{B}\dot{\mathbf{a}} + (h + \mathbf{n}^T\mathbf{D}\mathbf{n})\mathbf{h}\mathbf{h}^T\dot{\mathbf{A}} + c\mathbf{q}\mathbf{q}^T\dot{\mathbf{A}}]\,dV \tag{80}$$

Stationarity requires that

$$\frac{\partial F}{\partial \dot{\mathbf{a}}} = \mathbf{0} \quad \text{and} \quad \frac{\partial F}{\partial \dot{\mathbf{A}}} = \mathbf{0} \tag{81}$$

which precisely gives equation (32) with $\mathbf{K}_{aa}$, $\mathbf{K}_{a\lambda}$, $\mathbf{K}_{\lambda\lambda}$ and $\mathbf{f}_e$ as defined through equations (33), (34), (39) and (36).

It now remains to show that equation (77) indeed corresponds to the Euler equations

$$\mathbf{L}^{\mathrm{T}}\mathbf{D}(\dot{\boldsymbol{\varepsilon}} - \dot{\lambda}\mathbf{n}) = \mathbf{0} \tag{82}$$

$$\mathbf{n}\mathbf{D}^{\mathrm{T}}\dot{\boldsymbol{\varepsilon}} - (h + \mathbf{n}^{\mathrm{T}}\mathbf{D}\mathbf{n})\dot{\lambda} + c\nabla^2\dot{\lambda} = 0 \tag{83}$$

cf. equations (1), (2) and (16). To this end we first require that F be stationary with respect to $(\dot{\mathbf{u}}, \dot{\lambda})$: $\delta F = 0$. This yields

$$\int_V [(\delta\dot{\boldsymbol{\varepsilon}} - \delta\dot{\lambda}\mathbf{n})^{\mathrm{T}}\mathbf{D}(\dot{\boldsymbol{\varepsilon}} - \dot{\lambda}\mathbf{n}) + h\dot{\lambda}\delta\dot{\lambda} + c(\nabla\dot{\lambda})^{\mathrm{T}}(\nabla\delta\dot{\lambda})]\,\mathrm{d}V - \int_S \delta\dot{\mathbf{u}}^{\mathrm{T}}\dot{\mathbf{t}}\,\mathrm{d}S = 0 \tag{84}$$

With aid of the divergence theorem we obtain

$$\int_V -\delta\dot{\mathbf{u}}[\mathbf{L}^{\mathrm{T}}\mathbf{D}(\dot{\boldsymbol{\varepsilon}} - \dot{\lambda}\mathbf{n})]\,\mathrm{d}V + \int_S \delta\dot{\mathbf{u}}(\dot{\boldsymbol{\Sigma}}\mathbf{n}_s - \dot{\mathbf{t}})\,\mathrm{d}S \tag{85}$$

$$+ \int_V -\delta\dot{\lambda}[\mathbf{n}^{\mathrm{T}}\mathbf{D}\dot{\boldsymbol{\varepsilon}} - (h + \mathbf{n}^{\mathrm{T}}\mathbf{D}\mathbf{n})\dot{\lambda} + c\nabla^2\dot{\lambda}]\,\mathrm{d}V + \int_{S_\lambda} c\delta\dot{\lambda}(\nabla\dot{\lambda})^{\mathrm{T}}\mathbf{n}_\lambda\,\mathrm{d}S_\lambda = 0 \tag{86}$$

$\boldsymbol{\Sigma}$ being the stress tensor in matrix form, and $\mathbf{n}_s$ and $\mathbf{n}_\lambda$ denoting the outward normal to the body and the plastic part thereof, respectively. S and S_λ are the boundaries of the body and its plastified part, respectively. From equations (85) and (86) we can identify the Euler equations (82) and (83), the normal boundary conditions

$$\delta\dot{\mathbf{u}} = \mathbf{0} \quad \text{or} \quad \dot{\boldsymbol{\Sigma}}\mathbf{n}_s = \dot{\mathbf{t}} \tag{87}$$

and the non-standard boundary conditions (38).

REFERENCES

1. Z. P. Bazant, T. Belytschko and T.-P. Chang, 'Continuum theory for strain softening', *J. Eng. Mech. ASCE*, **110**, 1666–1692 (1984).
2. Z. P. Bazant and G. Pijaudier-Cabot, 'Nonlocal continuum damage, localization instability and convergence,' *J. Appl. Mech. ASME*, **55**, 287–293 (1988).
3. R. de Borst, 'Bifurcations in finite element models with a nonassociated flow law,' *Int. j. numer. anal. methods geomech.*, **12**, 99–116 (1988).
4. R. de Borst, 'Numerical methods for bifurcation analysis in geomechanics,' *Ing.-Arch.*, **59**, 160–174 (1989).
5. R. de Borst, 'Simulation of localisation using Cosserat theory', in N. Bićanić and H. A. Mang (eds.), *Proc. 2nd Int. Conf. on Computer Aided Analysis and Design of Concrete Structures*, Pineridge Press, Swansea, U.K., 1990, pp. 931–944.
6. R. de Borst, 'Simulation of strain localisation: A reappraisal of the Cosserat continuum', *Eng. Comput.*, **8**, 317–332 (1991).
7. E. Cosserat and F. Cosserat, *Théorie des Corps Deformables*, Herman, Paris, 1909.
8. H.-B. Mühlhaus and I. Vardoulakis, 'The thickness of shear bands in granular materials', *Géotechnique*, **37**, 271–283 (1987).
9. H.-B. Mühlhaus, 'Continuum models for layered and blocky rock', in *Comprehensive Rock Engineering, Vol. 2: Analysis & Design Methods*, Pergamon Press, Oxford, 1991.
10. H.-B. Mühlhaus, R. de Borst and E. C. Aifantis, 'Constitutive models and numerical analyses for inelastic materials with microstructure', in G. Beer *et al.* (eds.), *Computer Methods and Advances in Geomechanics*, Balkema, Rotterdam, 1991, pp. 377–386.
11. H.-B. Mühlhaus and E. C. Aifantis, 'A variational principle for gradient plasticity', *Int. J. Solids Struct.*, **28**, 845–857 (1991).
12. H. M. Zbib and E. C. Aifantis, 'On the localization and postlocalization behavior of plastic deformation, I, II, III', Res. Mechanica, **23**, 261–277, 279–292, 293–305 (1988).
13. D. Lasry and T. Belytschko, 'Localization limiters in transient problems', *Int. J. Solids Struct.*, **24**, 581–597 (1988).
14. H. L. Schreyer and Z. Chen, 'One-dimensional softening with localization', *J. Appl. Mech. ASME*, **53**, 791–979 (1986).
15. Z. Chen and H. L. Schreyer, 'Simulation of soil–structure interfaces with non-local constitutive models', *J. Eng. Mech. ASCE*, **113**, 1165–1677 (1987).

16. R. de Borst and P. H. Feenstra, 'Studies in anisotropic plasticity with reference to the Hill criterion', *Int. j. numer. methods eng.*, **29**, 315–336 (1990).
17. M. Ortiz and J. C. Simo, 'An analysis of a new class of integration algorithms for elastoplastic constitutive relations', *Int. j. numer. methods eng.*, **23**, 353–366 (1986).
18. K. Runesson, A. Samuelsson and L. Bernsprang, 'Numerical technique in plasticity including solution advancement control', *Int. j. numer. methods eng.*, **22**, 769–788 (1986).
19. J. C. Simo and R. L. Taylor, 'Consistent tangent operators for rate-independent elasto-plasticity', *Comp. Methods Appl. Mech. Eng.*, **48**, 101–118 (1985).
20. L. J. Sluys and R. de Borst, 'Strain softening under dynamic loading conditions', in N. Bićanić and H. A. Mang (eds.), *Proc. 2nd Int. Conf. on Computer Aided Analysis and Design of Concrete Structures*, Pineridge Press, Swansea, U.K., 1990, pp. 1091–1104.
21. L. J. Sluys and R. de Borst, 'A numerical study of concrete fracture under impact loading', in S. P. Shah *et al.* (eds.), *Micromechanics of Failure of Quasi-Brittle Materials*, Elsevier Applied Science, London, 1990, pp. 524–535.
22. J. C. Simo, 'Strain softening and dissipation: a unification of approaches', in J. Mazars and Z. P. Bazant (eds.), *Cracking and Damage: Strain Localization and Size Effect*, Elsevier Applied Science, London, 1989, pp. 440–461.
23. L. P. Kubin and J. Lépinoux, 'The dynamic organization of dislocation structures', in *Proc. Eighth Int. Conf. on Strength of Metals and Alloys*, Tampere, Finland, 1988, pp. 35–59.
24. J. Kratochvil, 'Dislocation pattern formation in metals', *Revue Phys. Appl.*, **23**, 419–429 (1988).
25. A. Franek, J. Kratochvil, J. Saxlová and R. Sedlácek, 'Synergetic approach to work hardening of metals', *Mater. Sci. Eng.*, **A137**, 119–123 (1991).
26. D. Walgraef and E. C. Aifantis, 'On the formation and stability of dislocation patterns, I–III', *Int. J. Eng. Sci.*, **12**, 1351–1372 (1985).
27. H.-B. Mühlhaus and J. Boland, 'A gradient plasticity model for Lüders band propagation', *Pure Appl. Geophys.*, in press.
28. Y. Estrin and L. P. Kubin, 'Plastic instabilities: phenomenology and theory', *Mater. Sci. Eng.*, **A137**, 125–134 (1991).